26839 DUP

GM87AP-000-511-G
CNRC 26839

EFFECT OF DEFORMATION ON THE AUSTENITE TO FERRITE TRANSFORMATION IN A PLAIN CARBON AND TWO MICROALLOYED STEELS

E. Essadiqi* and J.J. Jonas
Department of Metallurgical Engineering
McGill University
3450 University Street, Montreal, Canada H3A 2A7

ABSTRACT

Isotherma[illegible]pression tests were carried out on a plain C, and on a Mo as well as a Mo-Nb-V microalloyed steel in order to study the effect of deformation on the austenite to ferrite transformation. Dynamic TTT (DTTT) curves were established for the three steels; these show clearly the extent to which deformation accelerates the decomposition of austenite. This effect is reduced by the addition of the alloying elements Mo, Nb and V. It also decreases with increasing temperature. The substitutional elements Mo, Nb and V appear to reduce the nucleation rate through reduction of the austenite grain boundary energy. The growth rate is also reduced by these elements, apparently through the solute drag-like effect. The microstructural results indicate that the ferrite formed under dynamic conditions becomes more homogeneous and finer when the strain rate or the temperature is increased. Under static conditions, increasing the prestrain or the prestraining strain rate accelerates the γ-to-α transformation and reduces the mean grain size of the ferrite, although the highest transformation rate is still associated with the dynamic case.

*Now at the Industrial Materials Research Institute
75, boul. De Mortagne, Boucherville, Quebec J4B 6Y4

EFFECT OF DEFORMATION ON THE AUSTENITE TO FERRITE TRANSFORMATION IN A PLAIN CARBON AND TWO MICROALLOYED STEELS

1. INTRODUCTION

It is well known that the deformation of austenite in the temperature range where recrystallization is retarded increases the rate of ferrite formation (1-10). Such deformation also improves the mechanical properties of microalloyed steels which have been finish rolled at temperatures below the Ar_3,i.e. in the austenite plus ferrite, two phase range (11-15). This improvement is primarily due to the refinement of the ferrite grain size attributable to austenite pancaking; additional contributions are made by work hardening and recovery of the deformed ferrite and by the development of the {001} texture, which lowers the impact transition temperature (11).

The present study was undertaken with the objective of determining the effect of deformation on the isothermal austenite to ferrite transformation in a plain C and two microalloyed steels. Experiments were carried out under dynamic conditions in order to study the effect of strain and strain rate on the formation of ferrite during deformation. A second set was carried out under static conditions with different prestrains and prestraining strain rates. In this way, the effect of the alloying additions on the kinetics and morphology of ferrite formation could be determined in some detail. The influence of temperature and strain rate on the ferrite

microstructure was also established, and in particular, the manner in which temperature increase *refines* the ferrite structure.

2. MATERIALS AND EXPERIMENTAL PROCEDURE

The chemical compositions of the three steels studied are listed in Table I. Compression samples 11.43 mm in height and 7.62 mm in diameter were machined from the as-received plates, with their longitudinal axes parallel to the rolling direction. Specimens were first normalized at 1000°C to eliminate the rolling texture. They were subsequently annealed for 30 min at 1030 (plain C), 1060 (Mo steel), and 1100(Mo-Nb-V steel) °C and then quenched. This treatment ensured the dissolution of the Nb(CN) and V(CN) particles present at room temperature and produced an austenite grain size of about 100 μm (16, 17). Each sample was then reheated into the austenite region for 5 min (930°C for the plain C and Mo steels, and 1030°C for the Mo-Nb-V steel) and cooled to the test temperature at about 1°C/s. At the completion of the latter procedure, each of the three steels exhibited a grain size of around 25 μm.

TABLE I Chemical Compositions (wt.%) of the Materials Tested

Steel	C	Mn	Si	Al	Mo	Nb	V
Plain C	.06	1.42	.24	.025	-	-	-
Mo	.05	1.34	.20	.065	.29	-	-
Mo-Nb-V	.06	1.16	.20	.030	.30	.035	.115

Isothermal compression tests were carried out on an Instron machine modified for constant strain rate testing (18). A first series of tests was conducted at a strain rate of 7.4×10^{-4} s^{-1} in the temperature range from 790 to 840°C for the plain C and Mo steels and from 800 to 880°C for the Mo-Nb-V steel. A prestrain of $\varepsilon = 0.10$ was applied at a higher strain rate (7.4×10^{-2} s^{-1}), after which the strain rate was reduced to 7.4×10^{-4} s^{-1}, without unloading, for all the steels and at all the testing temperatures. In order to follow the transformation of the austenite into polygonal ferrite, the specimens were water quenched at the end of each test, the quench time for this operation being about 3s.

The effect of strain rate on the characteristics of the γ-to-α transformation was investigated in a second series of tests. In this case, the plain C and Mo steels were deformed at 800°C to total strains of $\varepsilon = 0.8$ at the following strain rates 7.4×10^{-1}, 7.4×10^{-2}, 7.4×10^{-3} and 7.4×10^{-4} s^{-1}. At the end of each test, the sample was immediately quenched.

In a third series of tests, the effect of the amount of predeformation and of the prestraining strain rate on the γ-to-α transformation was determined under *static* conditions. For this purpose, isothermal tests were performed on unstrained samples of the Mo steel at 800°C, as well as on samples given prestrains of 0.1 and 0.2. Two different prestraining strain rates (7.4×10^{-2} and 7.4×10^{-1} s^{-1})

were employed; the specimens were then held for increasing holding times before being quenched.

All the test samples were sectioned parallel to the deformation axis and polished for optical examination. Two different etchants were used: the polished samples were first etched with a 3% nital solution for 10 to 15 seconds in order to reveal the ferrite grain boundaries; they were further etched with a solution consisting of 10g of $Na_2S_2O_5$ in 100 ml of H_2O for 5 to 10 s (19) in order to enhance the contrast between the ferrite and martensite. The volume fraction of ferrite was determined using standard point counting procedures (20, 21).

3. RESULTS

Flow Curves

The appearance of the flow curves produced by the strain rate change technique can be seen in Figures 1 to 3. During the first part of each test, work hardening takes place, but is progressively overcome by dynamic recovery. The latter process, which is thermally activated, leads to flow stresses which depend on strain rate and temperature (as well as on the strain) in a manner which can be correlated with the Zener-Hollomon parameter Z that describes the experiments. The latter is equal to:

$$Z = \dot{\varepsilon} \exp(Q/RT)$$

where Q is the experimental activation energy, $\dot{\varepsilon}$ is the strain rate and T is the absolute temperature of deformation. The flow stress increases with Z, but not quite linearly.

After the strain rate decrease, the stress dropped abruptly due to the sudden decrease in the Z parameter (22). On continued straining following the strain rate change, the flow stress continued to rise, due to work hardening, until it reached a maximum, after which it dropped as a result of the austenite to ferrite transformation. When the three figures are compared, it is evident that the time (i.e., deformation) to the peak of the flow curve *increases* with the temperature of the test. This indicates that the transformation is initiated more and more slowly as the Ae_3 temperature is approached. Before the peak, the highest flow stress is associated with the lowest temperature, in the normal way. By contrast, at large strains, the lowest flow stress is observed to correspond to the *lowest* temperature. This is because the amount of flow softening after the stress peak increases as the test temperature is decreased for the following two reasons:

i) the flow stress of the α phase, at a given temperature, is lower than that of the γ phase with the same composition; and

ii) the volume fraction of α that is stable increases progressively as the test temperature is reduced.

Because of the lower flow stress of the α phase, the rate of flow softening can be related to the rate of the gamma to alpha transformation (12, 23). At a given temperature, the rate of softening decreases progressively as the strain increases. This has two causes: a) the kinetics of the austenite-to-ferrite transformation slow down because the driving force for the phase change decreases as the volume fraction of ferrite present approaches the equilibrium value; b) as the deformation increases, the transformed ferrite and the untransformed austenite both work harden progressively.

A further aspect of the flow curves for the plain C steel shown in Figure 1 is worthy of comment here. At 840°C, the curve has two unusual features: first, the stress level is lower than that at 820°C at any deformation; second, it displays multiple peaks or stress oscillations. This behaviour is due to the initiation of dynamic recrystallization in the gamma phase. The multiple peaks are related to the coarsening of the austenite grains during cycles of recrystallization (24, 25). The flow curves for the Mo-Nb-V steel shown in Figure 3 display limited evidence for dynamic recrystallization. The flow curve at 880°C is lower than that at 860°C. This should be compared with the 820 and 840°C curves of Figure 1. It appears that the softening at 880°C is due in part to the formation of ferrite and in

part to dynamic recrystallization of the austenite. The temperature decrease leads to an inhibition of the process of dynamic recrystallization. At 800°C and 0.8 of deformation (i.e. 954 s), the level of stress is equal to that at 820°C for the same deformation (i.e. time), even though the volume fraction of ferrite at 800°C is higher than that at 820°C. This effect is due to the following factors:

i) The amount of work hardening experienced by the austenite and the ferrite increases with decreasing temperature; and

ii) Dynamic precipitation of V(CN) increases the net work hardening rate of the ferrite.

The flow curves for the Mo steel shown in Figure 2 indicate that dynamic recrystallization is not occurring in the temperature range considered. It is retarded or prevented entirely due to the effect of Mo as a substitutional solute in retarding grain boundary motion (26). Finally, it should be added that the interpretation concerning the occurrence of dynamic recrystallization in the plain C steel at 840°C and in the ternary steel at 880°C suggests that dynamic recrystallization can be expected to occur in the Mo steel as well if the testing temperature is raised to the range 860 to 870°C.

Metallographic Results

Some examples of the microstructures encountered in the plain C steel are presented in Figure 4. These micrographs were chosen to illustrate the progress of the austenite-to-ferrite transformation during straining at 790°C. They indicate how the structure develops during the time interval between 14 and 954 s. They show clearly that polygonal ferrite starts to form at grain boundaries (corners and edges) and at some grain faces. Once the transformation has begun, further nucleation occurs at the untransformed grain boundaries. As the time (i.e. strain) increases, some ferrite grains are additionally nucleated inside the austenite grains, within deformation bands and perhaps at sub-boundary sites as well. It should be noted that all the original grain boundaries become saturated with ferrite grains at around 400 s (i.e., $\varepsilon = 0.4$), Figure 4c. The grains are relatively fine and are far from uniform in size (2 to 16 μm), reflecting the influence of the different classes of nucleation sites, their varying nucleus densities, and the different times available for their growth. It is evident that the ferrite grains are elongated along the perpendicular to the compression axis as a result of the deformation. After the completion of nucleation, the ferrite grains continue to grow but at a decreasing rate, because the austenite becomes more and more stable and the driving force for the transformation decreases. In the case of the Mo and Mo-Nb-V steels,

the evolution of the transformed microstructure was similar to that illustrated in Figure 4.

The effect of temperature on the structure of the transformed ferrite is illustrated in Figure 5 for the Mo steel. It can be seen from these micrographs that the grain size of the ferrite is *reduced* (see Table II) and the structure becomes more and more homogeneous as the temperature is increased. This can be attributed to the increase in the amount of deformation experienced by the sample before transformation begins as the temperature is increased. Furthermore, the ferrite growth rate is also reduced as the temperature is increased. Increasing the deformation prior to the appearance of the ferrite results in an increase in the nucleus density, so the grain size of the ferrite that forms decreases with increasing temperature.

Dynamic TTT Curves

The dynamic TTT curves pertaining to the plain C steel determined in the present study are presented in Figure 6. Those for the Mo and Mo-Nb-V steels are illustrated in Figures 7 and 8, respectively. They indicate how the volume fraction of ferrite evolves with time and temperature. The Ae_3 temperatures were calculated from the equilibrium model (27) and are collected in Table III for the three steels. The numbers above the dots indicate the actual volume fractions of ferrite measured by metallography. The PFs Dyn lines

(start of polygonal ferrite formation under dynamic conditions) correspond to the 'start time' for the formation of ferrite which, by convention, is considered to be associated with the presence of 5% ferrite. The upper parts of the DTTT curves have the classical C shape. The nose temperatures are apparently lower than any of the test temperatures. The static TTT curves were established by standard dilatometric techniques* and are reproduced on these diagrams in the form of dashed lines for comparison purposes.

The volume fraction of ferrite produced from austenite at a constant holding temperature gradually approaches the equilibrium value at long holding times. The equilibrium alpha fractions are marked on the vertical axes on the right side of these diagrams. These were calculated from the equilibrium model (27). The DTTT curves for the three steels show clearly the extent to which deformation accelerates the decomposition of austenite. Because of the acceleration, the PFs temperature associated with a fixed time is appreciably higher for the dynamic than for the conventional TTT curves. The difference between these PFs temperatures decreases, however, as the time required to initiate the transformation (i.e. the temperature) is increased. For the plain C steel, this difference decreases from 48 to 9°C

*The authors are indebted to Dr. Laurie Collins of PMRL, CANMET, EMR, Ottawa for providing them with these results.

in the range 50 to 500 s, respectively. For the Mo steel, the differences are 46 and 9°C at 60 and 1000 s, respectively. Finally, for the Mo-Nb-V steel, the differences are 54 and 5°C at 5 and 100 s, respectively.

In a similar manner, the PFs time associated with a fixed temperature is shorter for the dynamic than for the static TTT curves. However, the ratio of the PFs static to dynamic times decreases as the temperature is increased. The ratios for the plain C steel are 18 and 6 for 790 and 840°C, respectively. For the Mo steel, this ratio decreases from 14 to 5 as the temperature is increased from 790 to 840°C; for the Mo-Nb-V steel, the equivalent ratios are 8 and 1 for 800 and 880°C, respectively.

TABLE II The Mean Ferrite Grain Size at Different Temperatures in the Deformed ($\varepsilon = 0.8$) Plain C, Mo and Mo-Nb-V Steels

Steel	Testing Temperature/Mean Grain Size*				
Plain C	T°C	790	800	820	840
	$D_\alpha \mu m$	6.7	5	4	3.6
Mo	T°C	790	800	820	840
	$D_\alpha \mu m$	7.6	5.5	4	3.2
Mo-Nb-V	T°C	800	820	840	860	880
	$D_\alpha \mu m$	7.5	5.6	5	4.5	3.5

* The relative error in these measurements is ± 15 %.

TABLE III Equilibrium Ae_3 Temperatures for the Plain C, Mo and Mo-Nb-V Steels.

Steel	A_{e_3} Temperature, °C
Plain C	850
Mo	885
Mo-Nb-V	900

Effect of Strain Rate on Dynamic Transformation

The effect of strain rate on the structure of ferrite formed dynamically is illustrated in Figure 9 for the Mo steel at 800°C. At the highest strain rates, the structures consist of polygonal ferrite, martensite (i.e., transformed austenite) and some acicular ferrite formed during quenching because of the instability of the deformed austenite. The polygonal ferrite is very fine ($\simeq$ 2 μm) and represents an unusually high nucleus density. As the strain rate is decreased, the ferrite grains increase in size, heterogeneity and volume fraction. As the strain rate is decreased from 7.4×10^{-1} to 7.4×10^{-4} s^{-1}, the time for dynamic transformation, which corresponds to the attainment of a strain of 0.8, increases from 1 to 1170 s.

Transformation Under Static Conditions

The effect of prior deformation on the austenite to ferrite transformation under static conditions is shown in Figure 10 for the Mo steel. The progress of ferrite formation during deformation (i.e. for the dynamic case) is reproduced for comparison purposes on the same figure. As the prestrain is increased from 0 to 0.2, the amount of ferrite present at a given time increases, although it remains less than that formed during deformation (i.e. dynamically). The rate of the austenite to ferrite transformation also increases with the prestrain in the static

case, although these remain below those associated with dynamic transformation.

The effect of strain rate on the transformation is illustrated by the two curves pertaining to the same prestrain, $\varepsilon = 0.20$, and to two different strain rates, $\dot{\varepsilon} = 7.4 \times 10^{-2}$ and 7.4×10^{-1} s^{-1}. Increasing the strain rate increases the volume fraction of ferrite present, although the effect is small, amounting to a few percent.

Selected structures pertaining to the static austenite to ferrite transformation are presented in Figure 11. These represent the effect of increasing prestrain (Figures 11a to c) and increasing strain rate (Figures 11c and d); all the structures correspond to a holding time of 1000 s prior to quenching. The micrograph of the material transformed from the undeformed sample shows that the ferrite is nucleated predominantly at the corners and edges of the austenite grains, and to a lesser extent at the grain faces. The number of nuclei in the absence of deformation is not large; accordingly, the grain size of the ferrite is about 12 μm. As the prestrain is increased, the number of nuclei also increases and the grain size is reduced, for example, to 8 μm in the case of the sample prestrained to $\varepsilon = 0.20$ and held for 1000 s (Figure 11c). When the prestraining strain rate is increased by one order of magnitude, the ferrite grain size is further reduced to 7 μm, as can be seen from Figures 11c and 11d. From these figures, it is also apparent that the strain rate increase is more effective in raising the nucleus

density than in modifying the volume fraction of ferrite present at a given time. In all cases, the structure produced under static conditions is more homogeneous than that obtained in the dynamic case from the tests at low strain rate.

4. DISCUSSION

It is clear from the results presented above that straining accelerates the γ-to-α transformation. For example, deformation advances the positions of the dynamic PFs lines with respect to the static PFs curves by up to an order of magnitude. This accelerating effect is due to a number of factors:

i) As a consequence of the change in the shape of the austenite grains, there is an increase in S_V, the grain boundary area per unit volume;

ii) Straining also leads to the formation of deformation bands (28,29), which also contain a number of nucleation sites;

iii) There appears to be an increase in the interfacial energy of annealing twins (30) brought about by austenite deformation, a change which again increases the probability of nucleation.

The detailed mechanisms by which deformation increases the nucleation rate of ferrite have been studied by several authors. For example, Sandberg and Roberts (2, 3) have proposed that the prolific nucleation of ferrite in deformed austenite is associated with the bulges formed by local austenite grain boundary migration. Amin and Pickering (5) have suggested that the increased nucleation rate of ferrite at deformed austenite grain boundaries is due to the formation of subgrains near the boundaries. Tamura and Umemoto (31) have proposed that the strain energy of the dislocations stored in deformed austenite raises the energy of the latter and favors ferrite nucleation within deformed austenite in this way. The effect of deformation on the nucleation process will now be examined in more detail.

Dynamic Austenite To Ferrite Transformation

In the present case, the maximum nucleation rate of ferrite for the three steels increased as the temperature was decreased (23). This is due to the concurrent increase in the driving force for transformation. The structure of the ferrite produced at low strain rate (7.4×10^{-4} s^{-1}) by dynamic transformation was heterogeneous in grain size (2 - 16 μm). This is presumably because the grains are not nucleated at the same time and under the same conditions. Thus each grain has a different growth time and appears in a region with a different nucleus density.

Increasing the strain rate was also effective in accelerating the nucleation rate. In the case of the Mo steel at 800°C, as the strain rate was increased from 7.4×10^{-4} to 7.4×10^{-1} s^{-1}, the nucleation rate increased by about two orders of magnitude. This is due to the increase in the strain at a given time, which increases with strain rate. It has been reported by Desalos et al. (8) that, after the controlled rolling of low alloy steels, there is an increase in the ferrite nucleus density in deformed austenite. This could indicate that nucleation is enhanced when dislocations are absorbed on austenite grain boundaries. Increasing the strain rate also increases the homogeneity of the structure, leading to a very fine ferrite grain size ($\simeq 2$ μm).

Static Transformation

In the static case, the ferrite nucleation rate was increased by prestraining, and the ferrite grain size was more homogeneous. Increasing the strain rate was also effective in accelerating the nucleation rate. However, these increases are small compared to the effect of *concurrent* deformation. According to the results obtained on the Mo steel at 800°C, the nucleation rate in the dynamic case at a strain rate of 7.4×10^{-4} s^{-1} is about 30 times greater than in the static case. When the strain rate is increased by three orders of magnitude, the nucleation rate is raised by the same order. Thus the ferrite grain size is further reduced.

The Effect of Deformation on the TTT Curves

The effect of deformation on the PFs(static)/PFs(dynamic) ratio is illustrated in Figure 12. Here PFs(static) represents the ferrite start time in the absence of deformation, and the PFs(dynamic) data points are taken from the DTTT curves of Figures 6, 7 and 8. It is apparent that the ratio depends on temperature, and more particularly on the degree of supercooling below the Ae_3 temperature, Figure 13. The effect of composition on this ratio is also shown. As the level of the alloying additions is increased, the accelerating effect of deformation is decreased. This is related to the influence of the substitutional elements Mo, Nb and V on the ferrite nucleation and growth rates. As shown in more detail elsewhere (23), both rates are reduced by the above elements, so that the ferrite grain size is increased, as shown in Table III.

The effect of alloying on the ferrite nucleation rate described above is consistent with several earlier studies reported in the literature. For example, Aaronson et al. (32, 33) have shown that Mo retards the nucleation rate of ferrite; they concluded that Mo addition lowers the austenite grain boundary energy and thus increases the net interfacial free energy required to form a ferrite nucleus. In a similar manner, Ouchi et al. (29) noted that Nb addition retards transformation and explained this effect in terms of a decrease in the austenite grain boundary energy caused by the segregation of Nb to

these boundaries. Although the influence of V has not been studied in detail, it may also segregate to the γ/γ grain boundaries while in solution, reducing the interfacial energy, and thus decreasing the ferrite nucleation rate in a manner analogous to that of Mo and Nb addition described above.

The ferrite growth rate in the three steels tested was also found to be reduced by the alloying elements Mo, Nb and V. This effect increases with the degree of undercooling (Ae_3 - T), Figure 13. Some substitutional alloying elements influence austenite/ferrite interface motion through a solute drag-like effect, SDLE. The existence of this effect was suggested by Kinsman and Aaronson (34), as well as by Hillert (35). Recently, suggestions have been made that Cr, Mn, Mo, Ti and V affect the growth rate of ferrite by an SDLE (32, 36-38). In this approach, an alloying element that has an appreciable size misfit with respect to the Fe atom (austenite or ferrite) segregates to the disordered austenite/ferrite interface during growth and attracts carbon atoms. If the alloying element decreases the activity of carbon in austenite, it tends to collect carbon atoms, and so to reduce the concentration of carbon in the austenite in regions remote from itself. As the carbon concentration at the boundary is increased in this way, the growth kinetics are retarded. In this respect, Mo, Nb and V, which all exhibit size misfits relative to the iron atom, Table 4, and also decrease carbon activity, are expected to be effective in retarding the ferrite growth rate in the manner described above.

TABLE IV Atomic Size Difference with Respect to γ-Iron of Mo, Nb and V (39).

Symbol	r_x(A)	$(r_x-r_{fe})/r_{fe}$
Mo	1.400	0.15
Nb	1.468	.10
V	1.346	.06

Effect of Temperature

The effect of temperature on ferrite refinement in the dynamic case is related to the influence of the strain accumulated before the transformation and also to the decrease in growth rate as the temperature is increased. The latter phenomenon reduces the saturation effect of the grain boundaries and, combined with the effect of deformation, increases the potential nucleation sites available for ferrite on the untransformed austenite grain boundaries at large deformations. As the temperature is increased, the ferrite grain size is reduced (Table III), and the structure becomes more homogeneous. Such refinement of the structure is similar to that obtained in the dynamic case with high strain rates at lower temperatures. This similarity is related to the influence of deformation of the austenite prior to its decomposition. Thus the number of ferrite nuclei created

increases. Refinement of the ferrite grain size can be achieved in this way by increasing either the temperature or the strain rate.

5. CONCLUSIONS

As a result of this study, the following conclusions were reached.

1. In the dynamic tests, after the stress peak at the lower strain rate, the amount of flow softening observed increases as the test temperature is *decreased* because:

   i) At a given temperature, the flow stress of the alpha phase is lower than that of the gamma phase from which it forms;

   ii) The volume fraction of ferrite that is stable increases as the test temperature is decreased.

2. The DTTT curves for the three steels clearly show the extent to which deformation accelerates the decomposition of austenite. The PFs temperature associated with a fixed time is appreciably higher for the dynamic than for the conventional TTT

curves. For the plain C steel, the difference between these temperatures decreases from 48 to 9°C in the range 50 to 500 s, respectively. For the Mo and Mo-Nb-V steels, the differences are 46 and 9°C at 60 and 1000 s, and 54 and 5°C at 5 and 100 s, respectively. Similarly, the PFs time associated with a fixed temperature is shorter for the dynamic than for the static TTT curves. The ratio of the static to dynamic PFs times decreases as the temperature is increased. For example, the ratios for the plain C steel are 18 and 6 for 790 and 840°C, respectively. For the Mo steel, this ratio decreases from 14 to 5 as the temperature is increased from 790 to 840°C; for the Mo-Nb-V steel, the equivalent ratios are 8 and 1 for 800 and 880°C, respectively. The accelerating effect of deformation is thus seen to decrease as the level of alloying addition is increased. This is related to the influence of the substitutional elements Mo, Nb and V on the nucleation and growth rates.

3. The mean grain size of ferrite formed under dynamic conditions is reduced from about 7 to 3 μm as the temperature is *increased* in the range 790 to 840°C for the plain C and Mo steels and 800 to 880°C

for the Mo-Nb-V steel. This is because the deformation imposed on the austenite prior to its decomposition, and thus the number of ferrite nuclei created, increases with temperature. The homogeneity of the ferrite grain structure, which is relatively inhomogeneous at low temperatures and strain rates, also increases with temperature. The rate of ferrite formation increases markedly with strain rate; this is because the strain applied at a given time increases linearly with strain rate. The polygonal ferrite formed at the two highest strain rates (7.4×10^{-2} and 7.4×10^{-1} s-1) at a deformation of 0.8 is homogeneous in size and very fine (2 μm);

4. When the Mo steel is transformed under static conditions, the structure of the ferrite formed is homogeneous. The static process leads to grain sizes of about 10 μm. Increasing the static prestrain leads to more effective acceleration of the austenite to ferrite transformation than increasing the prestraining strain rate, although the highest transformation rates are still associated with the dynamic case.

ACKNOWLEDGEMENTS

The authors are indebted to Dr. L. Collins of the Physical Metallurgy Research Laboratories of CANMET, Energy, Mines and Resources, Ottawa, for providing the dilatometric transformation data. They also acknowledge with gratitude the assistance received from Dr. G.E. Ruddle of CANMET with respect to the provision of experimental materials. Finally, they are thankful to CANMET for financial support, as well as to the Natural Sciences and Engineering Research Council of Canada, the Quebec Ministry of Education (FCAR program), and the Canadian Steel Industry Research Association.

REFERENCES

1. K.J. Irvine, T. Goldman, J. Orr and B. Pickering: JISI, 1970, 208, pp. 717-726.

2. A. Sandberg and W. Roberts: "Thermomechanical Processing of Microalloyed Austenite", A.J. DeArdo, G.A. Ratz and P.J. Wray, Eds., TMS-AIME, Warrendale, PA, 1982, pp. 405-431.

3. W. Roberts, H. Lidefelt and A. Sandberg: " Hot Working and Forming Processes", C.M. Sellars and G.J. Davies, Eds., The Metals Society, London, 1980, pp. 38-42.

4. J.J. Jonas and R.A. do Nascimento: "Fundamentals of Dual Phase Steels", R.A. Kot and B.L. Bramfitt, Eds., TMS-AIME, Warrendale, PA, 1981, pp. 95-112.

5. R.K. Amin and F.B. Pickering: Ref. 2, pp. 377-403.

6. R. Priestner: Ibid., pp. 455-466.

7. M.J. Crooks, A.J. Garratt-Reed, J B. Vander Sande and W.S. Owen: Metall. Trans. A, 1982, 13A, pp. 1347-1353.

8. Y. Desalos, A. LeBon and R. Lombry: "Les Traitements Thermomécaniques: Aspects Théoriques et Applications", 24eme colloque de métallurgie, INSTN, Saclay, France, 1981, pp. 137-147.

9. R.W.K. Honeycombe: Metal Sci., 1980, 14, pp. 201-214.

10. M. Umemoto, H. Ohtsuka, H. Kato and I. Tamura: "High Strength Low Alloy Steels", D. P. Dunne and T. Chandra, Eds., Wollongong, Australia, 1984, pp. 107-112.

11. T. Hashimoto, H.Ohtani, T. Kobayashi, N. Hatano and S. Suzuki: Ref. 2, pp. 501-520.

12. E. Essadiqi, M.G. Akben and J.J. Jonas: "Phase Transformations in Ferrous Alloys", A.R. Marder and J.I. Goldstein, Eds., TMS-AIME, Warrendale, PA, 1984, pp. 391-395.

13. P. Bufalini and A. April: "Science and Technology of Flat Rolled Products" The Iron and Steel Institute of Japan, 1981, pp. 945-956.

14. T. Tanaka, N. Tabata, T. Hatomura and C. Shiga: "Microalloying 75", Union Carbide Corporation, New York, 1975, p. 107-118.

15. R. Speich and D.S. Dabkowski: "The Hot Deformation of Austenite", J.B. Ballance, Ed., AIME, Cleveland, Ohio, 1976, pp. 557-598.

16. B. Bacroix: M.Eng. Thesis, 1981, McGill University, Montreal.

17. T.V. Floros: M. Eng. Thesis, 1984, McGill University, Montreal.

18. M.J. Luton, J.P. Immarigeon and J. J. Jonas: J. Phys. E: Sci. Instr., 1974, 7, pp. 862-864.

19. A.M. Marder and A.O. Benscoter: Metallography, 1982, 15, pp. 73-85.

20. ANSI/ASTM Handbook E562-76.

21. H. Abrams: "Stereology and Quantitative Metallography", ASTM STP 504, American Society For Testing and Materials, 1972, pp. 138-182.

22. J.P. Immarigeon and J. J. Jonas: Acta Metall., 1971, 19, pp. 1053-1061.

23. E. Essadiqi: Ph. D. Thesis, 1986, McGill University, Montreal.

24. T. Sakai, M.G. Akben and J.J. Jonas: Ref. 2, pp. 237-252.

25. T. Sakai and J.J. Jonas: Acta Metall., 1984, 32, pp. 189-209.

26. M.G. Akben and J.J. Jonas: "Technology and Applications of HSLA Steels", ASM, Metals Park, Ohio, 1983, pp. 149-161.

27. K. Hashigushi, J. S. Kirkaldy, T. Fukuzumi and V.Pavaskar: McMaster University, Private Communication.

28. I. Kozasu, C. Ouchi, T. Sampei and T. Okita: "Microalloying 75", Union Carbide Corporation, New York, 1975, pp. 120-135.

29. C. Ouchi, T. Sampei and I. Kozasu: Trans. ISIJ, 1982, 22, pp. 214-222.

30. H. Inagaki: Trans. ISIJ, 1983, 23, pp. 1059-1067.

31. M. Umemoto and I. Tamira: Kyoto University, Japan, Private communication, 1985.

32. W.T. Reynolds, Jr, M. Enomoto and H.I. Aaronson: "Phase Transformations in Ferrous Alloys", A.R. Marder and J.I. Goldstein, Eds., TMS-AIME, Warrendale, PA, 1984, pp. 155-200.

33. H.I. Aaronson, H.A. Domian and G.M. Pound: Trans. AIME, 1966, 236, pp. 768-780.

34. K.R. Kinsman and H.I. Aaronson: "Transformation and Hardenability in Steels", Climax Molybdenum, Co., 1971, pp. 39-53.

35. M. Hillert: "The Mechanisms of Phase Transformation in Crystalline Solids", Inst. of Metals, London, Monograph, 1969, 33, pp. 231-247.

36. J.R. Bradley and H.I. Aaronson: Metall. Trans. A, 1981, 12A, pp. 1729-1741.

37. T. Abe, H I. Aaronson and G.J. Shiflet: Metall. Trans. A , 1985, 16A, pp. 521-527.

38. J.R. Bradley, G.J. Shiflet and H.I. Aaronson: "Solid-Solid Phase Transformations", H.I. Aaronson, Ed., TMS-AIME, Warrendale, PA, 1983, pp. 127-.

39. B. Bacroix, M.G. Akben and J.J. Jonas: Ref. 2, pp. 293-318.

FIGURE CAPTIONS

Figure 1 Flow curves produced at 840, 820, 800 and 790°C when the plain C steel was tested using the strain rate change technique. The oscillations at 840°C are due to the occurrence of dynamic recrystallization in the austenite.

Figure 2 Flow curves produced at 840, 820, 800 and 790°C when the Mo steel was tested using the strain rate change technique.

Figure 3 Flow curves produced at 880, 860, 840, 820 and 800°C when the Mo-Nb-V steel was tested using the strain rate change technique.

Figure 4 Microstructure of plain C steel samples deformed at 790°C and water quenched. (a) deformed for 14 s to $\varepsilon = 0.11$; 8% PF; (b) deformed for 73 s to $\varepsilon = 0.30$; 27% PF; (c) deformed for 409 s to $\varepsilon = 0.4$; 31% PF; (d) deformed for 954 s to $\varepsilon = 0.8$; 57% PF.

Figure 5 Microstructure of Mo steel samples deformed at $\dot{\varepsilon} = 7.4 \times 10^{-4}\ s^{-1}$ and water quenched. (a) deformed at 790°C for 954 s to $\varepsilon = 0.8$; 64% PF; (b) deformed at 800°C for 954 s to $\varepsilon = 0.8$; 52% PF; (c) deformed at 820°C for 954 s to $\varepsilon = 0.8$; 33% PF; (d) deformed at 840°C for 954 s to $\varepsilon = 0.8$; 13% PF.

Figure 6 TTT characteristics of the plain C steel.

Figure 7 TTT characteristics of the Mo steel.

Figure 8 TTT characteristics of the Mo-Nb-V steel.

Figure 9 Microstructure of Mo steel samples deformed at 800°C and water quenched. (a) deformed for 1 s to $\varepsilon = 0.8$ at a constant strain rate of 7.4×10^{-1} s^{-1}; 27% PF; (b) deformed for 11 s to $\varepsilon = 0.8$ at a constant strain rate of 7.4×10^{-2} s^{-1}; 34% PF; (c) deformed for 116 s to $\varepsilon = 0.8$ at a constant strain rate of 7.4×10^{-3} s^{-1}; 46.5% PF; (d) deformed for 1167 s to $\varepsilon = 0.8$ at a constant strain rate of 7.4×10^{-4} s^{-1}; 52% PF.

Figure 10 Effect of prestrain and strain rate on the austenite to ferrite transformation at 800°C in the Mo steel.

Figure 11 Microstructure of Mo steel samples held for 1000 s at 800°C and water quenched. (a) No deformation; 18%PF; (b) Prestrained to $\varepsilon = 0.10$ at $\dot{\varepsilon} = 7.4 \times 10^{-2}$ s^{-1}; 22% PF; (c) Prestrained to $\varepsilon = 0.20$ at $\dot{\varepsilon} = 7.4 \times 10^{-2}$ s^{-1}; 30% PF; (d) Prestrained to $\varepsilon = 0.20$ at $\dot{\varepsilon} = 7.4 \times 10^{-1}$ s^{-1}; 31% PF.

Figure 12 Effect of deformation on the polygonal ferrite start time for the plain C, Mo and Mo-Nb-V steels.

Figure 13 Effect of degree of undercooling on the polygonal ferrite start time in the three steels.

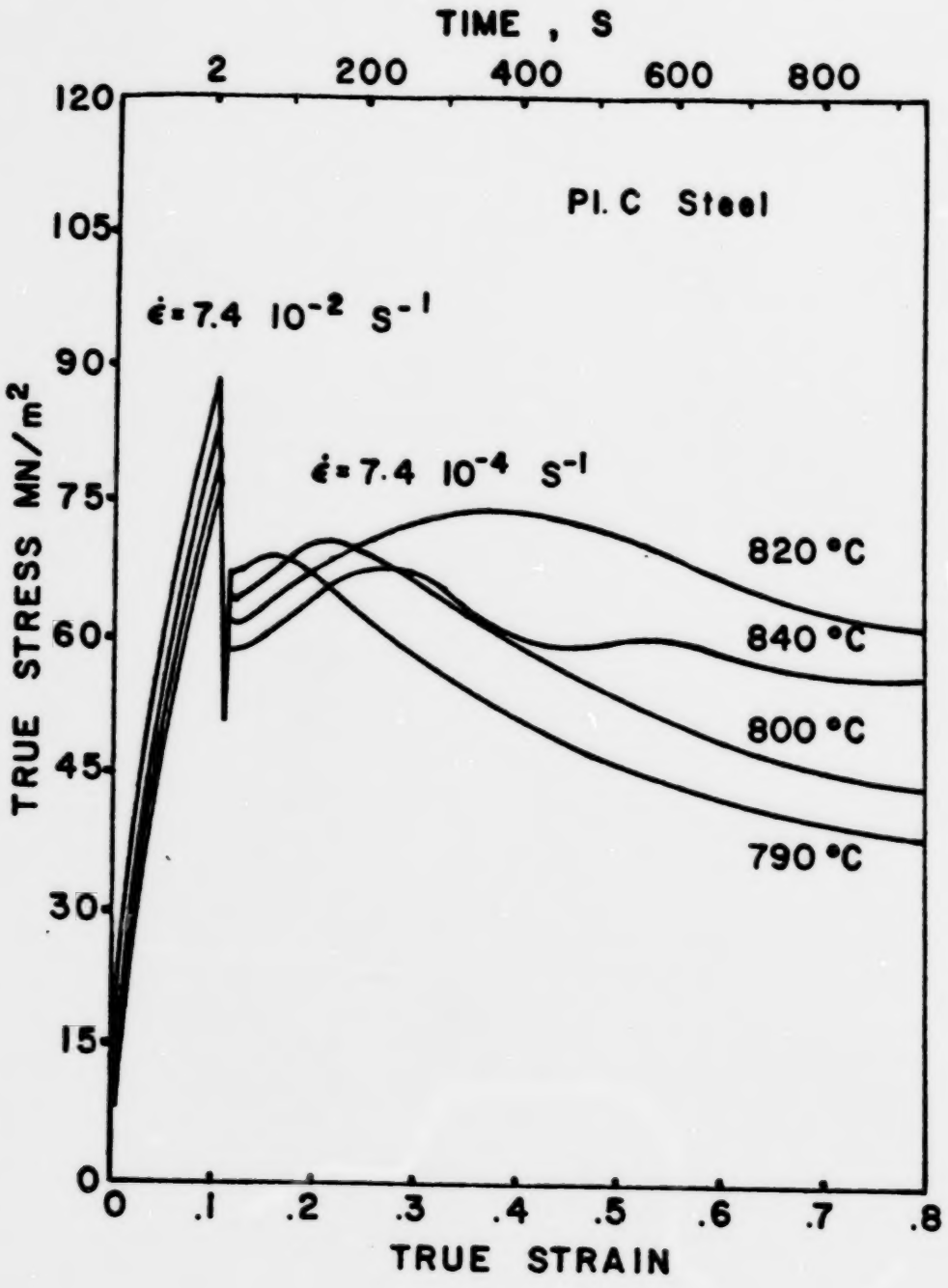

Figure 1 Flow curves produced at 840, 820, 800 and 790°C when the plain C steel was tested using the strain rate change technique. The oscillations at 840°C are due to the occurrence of dynamic recrystallization in the austenite.

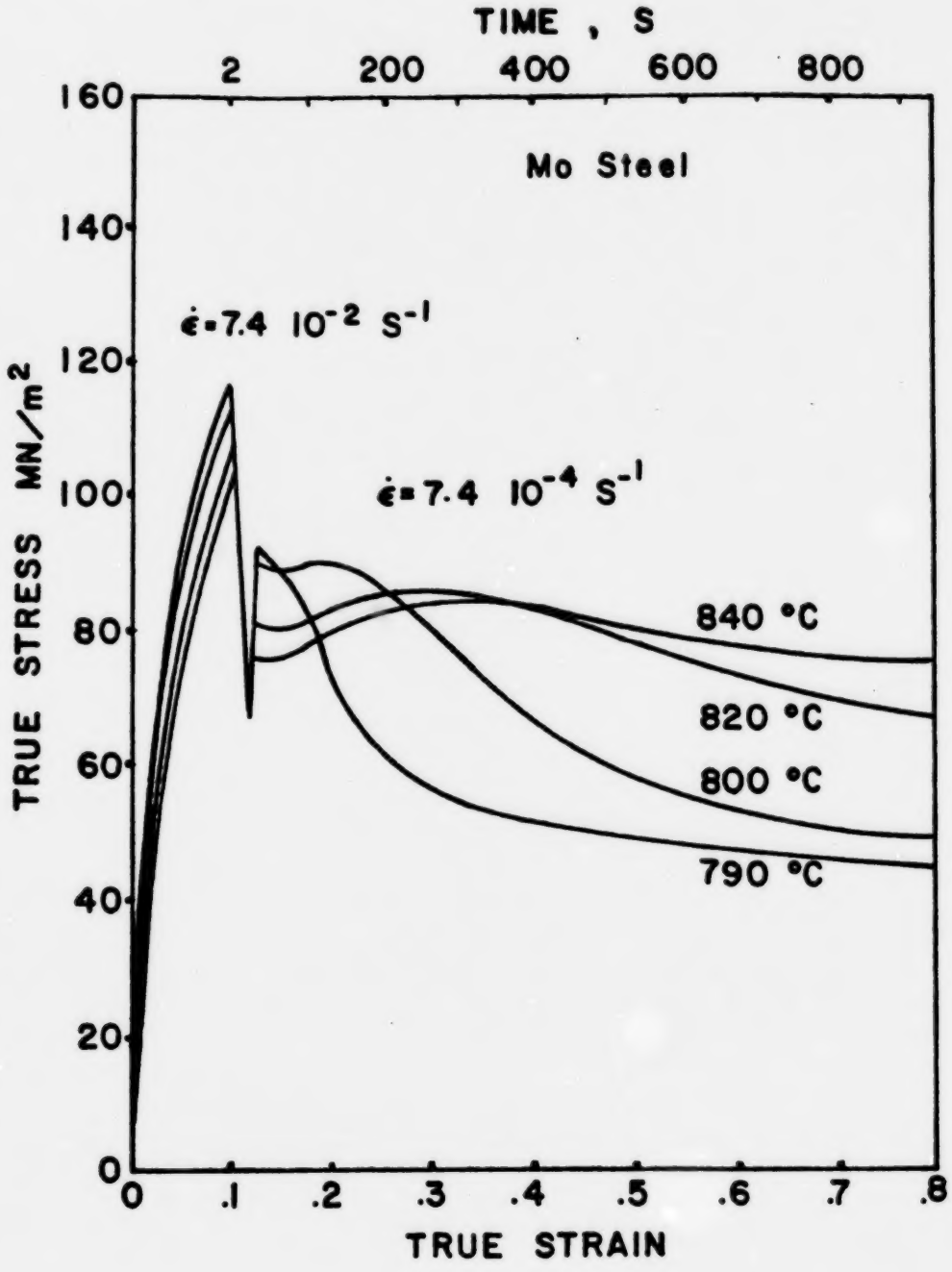

Figure 2 Flow curves produced at 840, 820, 800 and 790°C when the Mo steel was tested using the strain rate change technique.

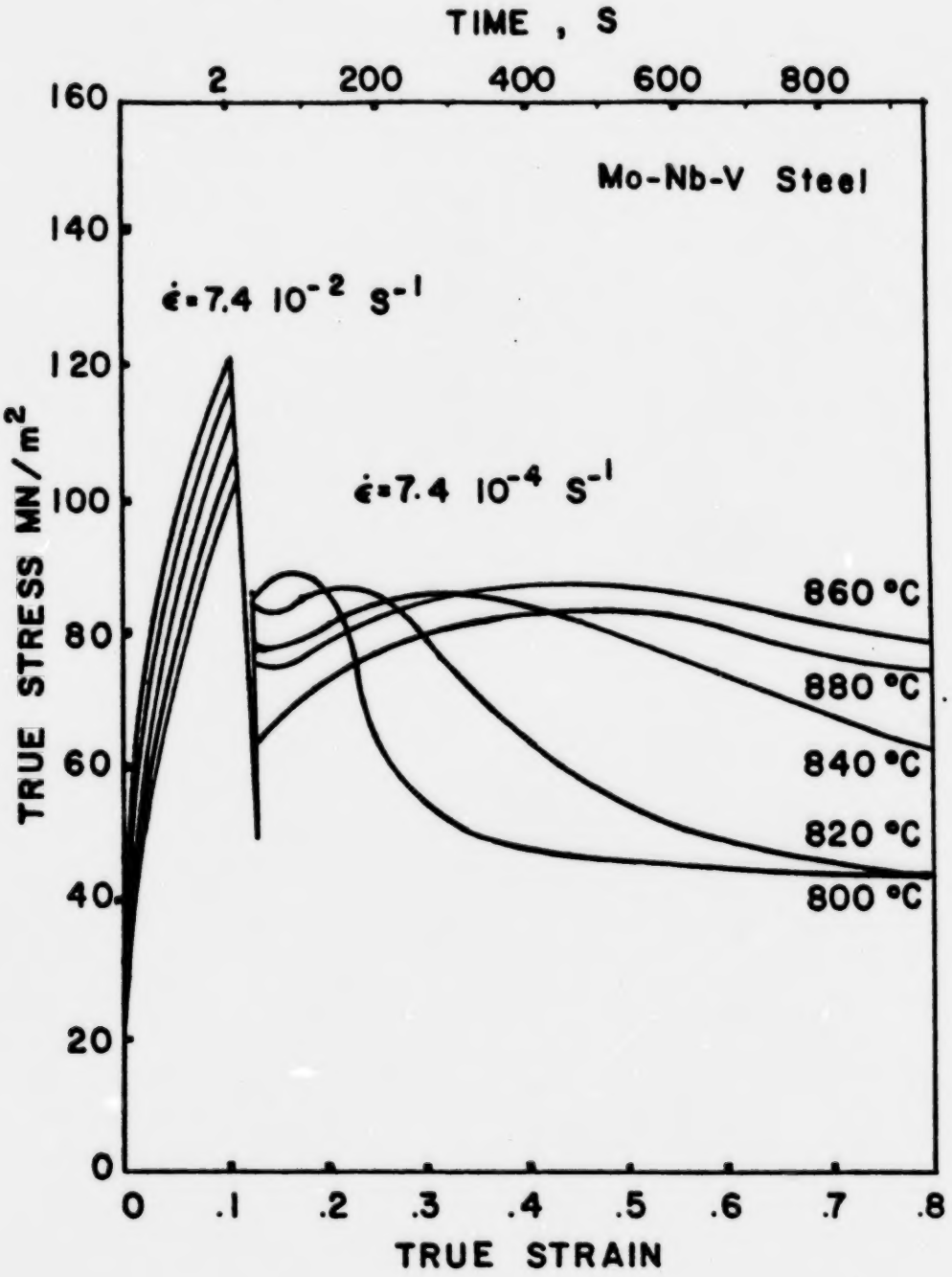

Figure 3 Flow curves produced at 880, 860, 840, 820 and 800°C when the Mo-Nb-V steel was tested using the strain rate change technique.

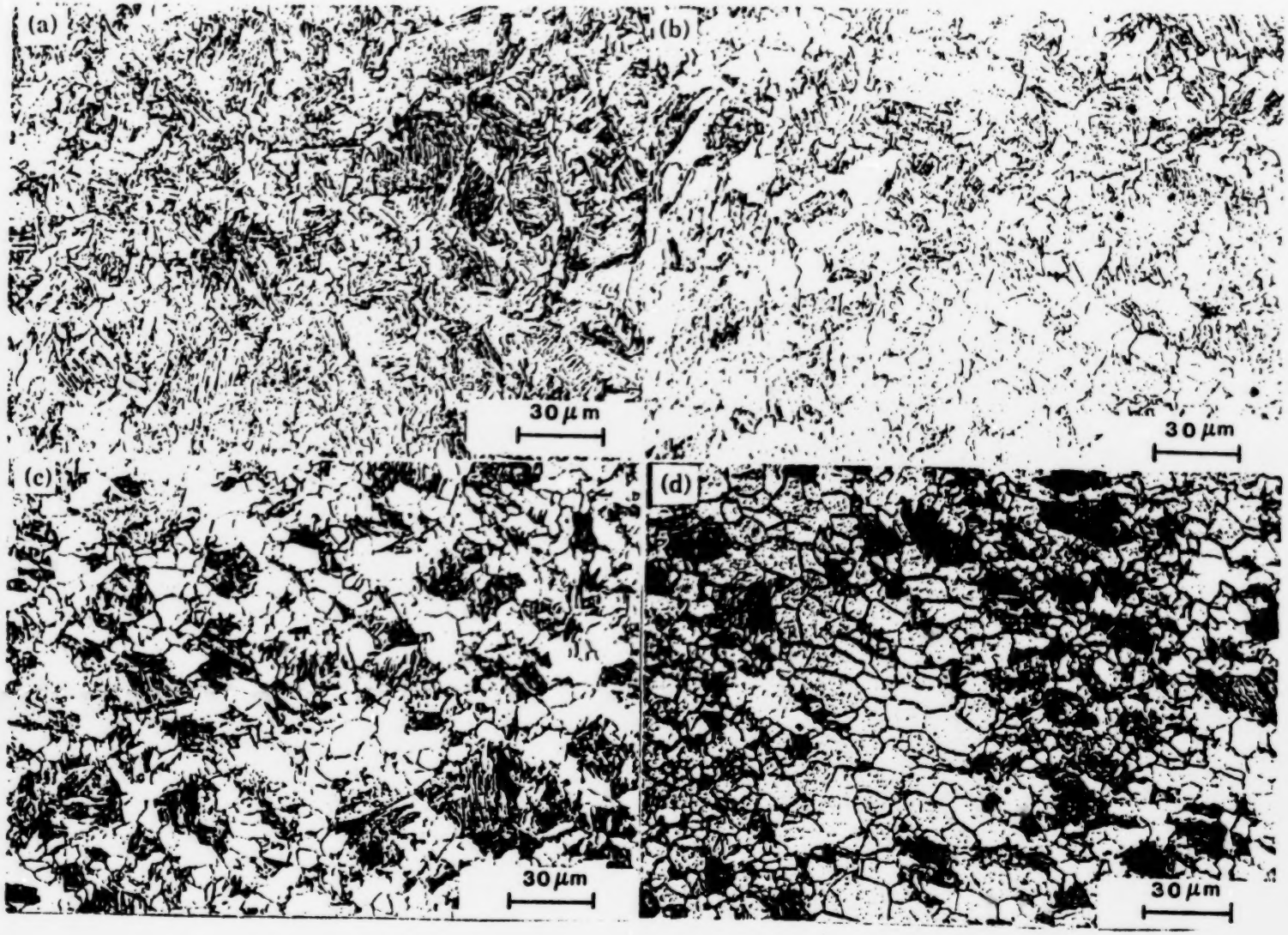

Figure 4 Microstructure of plain C steel samples deformed at 790°C and water quenched. (a) deformed for 14 s to $\varepsilon = 0.11$; 8% PF; (b) deformed for 73 s to $\varepsilon = 0.30$; 27% PF; (c) deformed for 409 s to $\varepsilon = 0.4$; 31% PF; (d) deformed for 954 s to $\varepsilon = 0.8$; 57% PF.

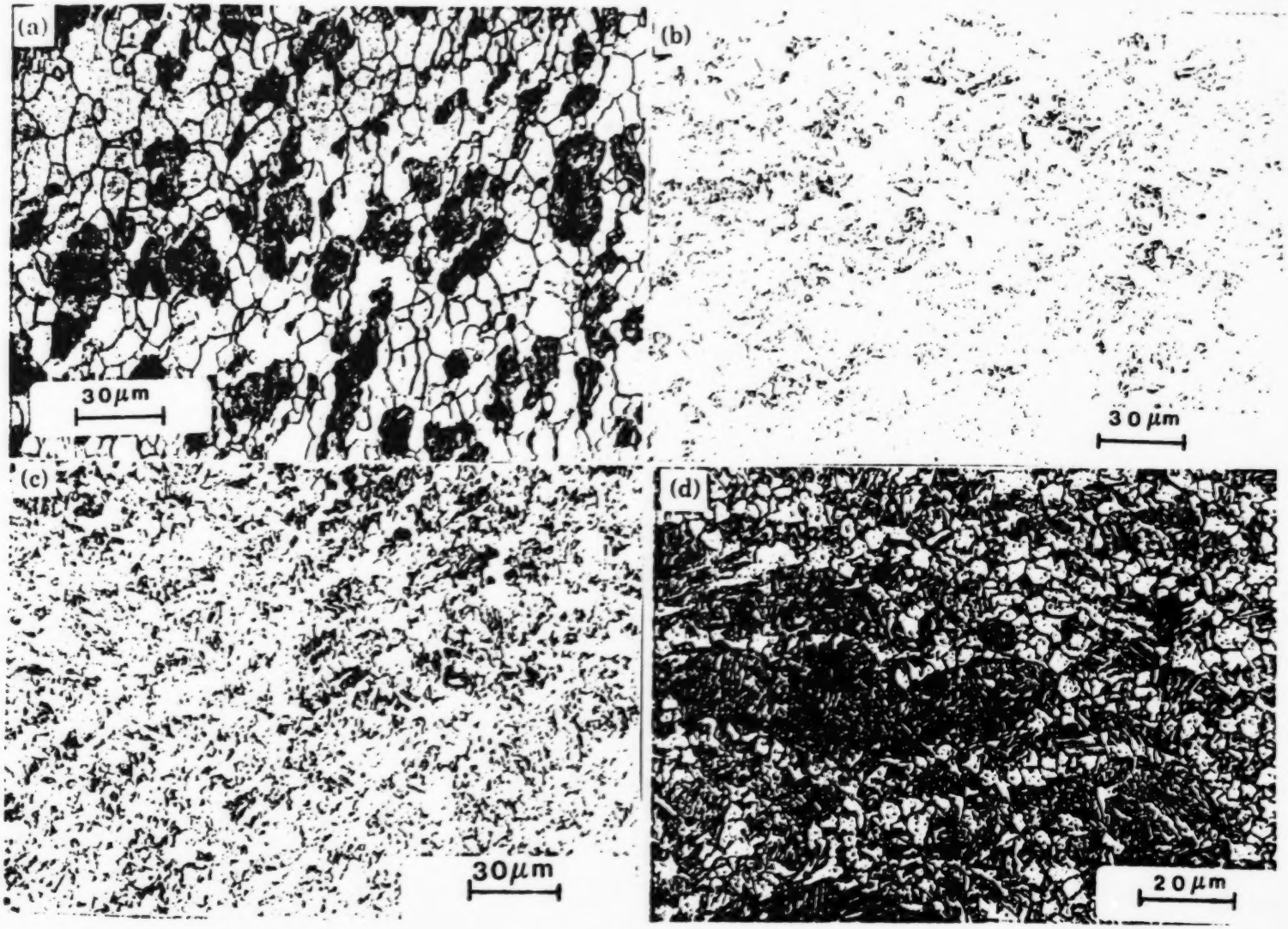

Figure 5 Microstructure of Mo steel samples deformed at $\dot{\varepsilon} = 7.4 \times 10^{-4}\ s^{-1}$ and water quenched. (a) deformed at 790°C for 954 s to $\varepsilon = 0.8$; 64% PF; (b) deformed at 800°C for 954 s to $\varepsilon = 0.8$; 52% PF; (c) deformed at 820°C for 954 s to $\varepsilon = 0.8$; 33% PF; (d) deformed at 840°C for 954 s to $\varepsilon = 0.8$; 13% PF.

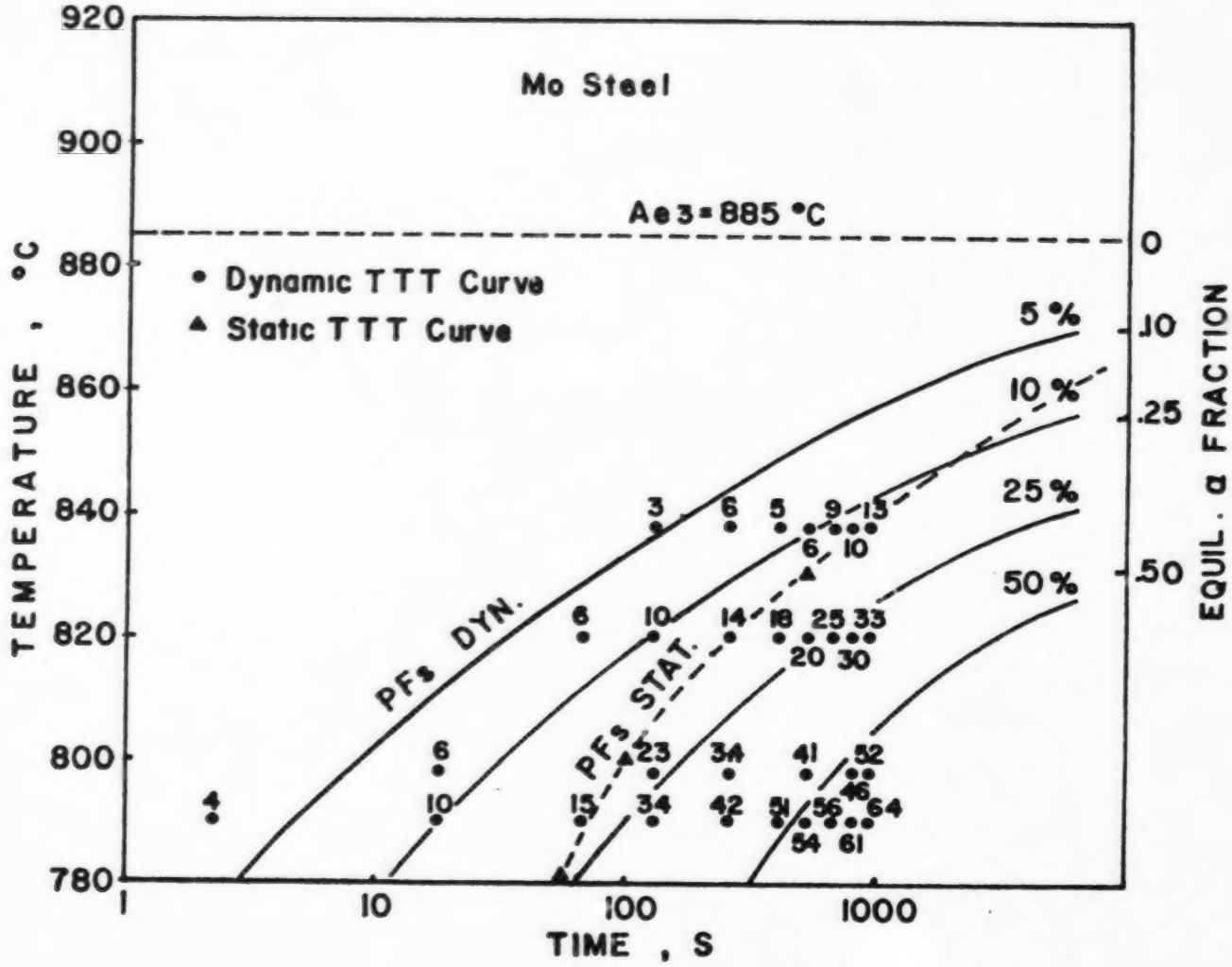

Figure 7 TTT characteristics of the Mo steel.

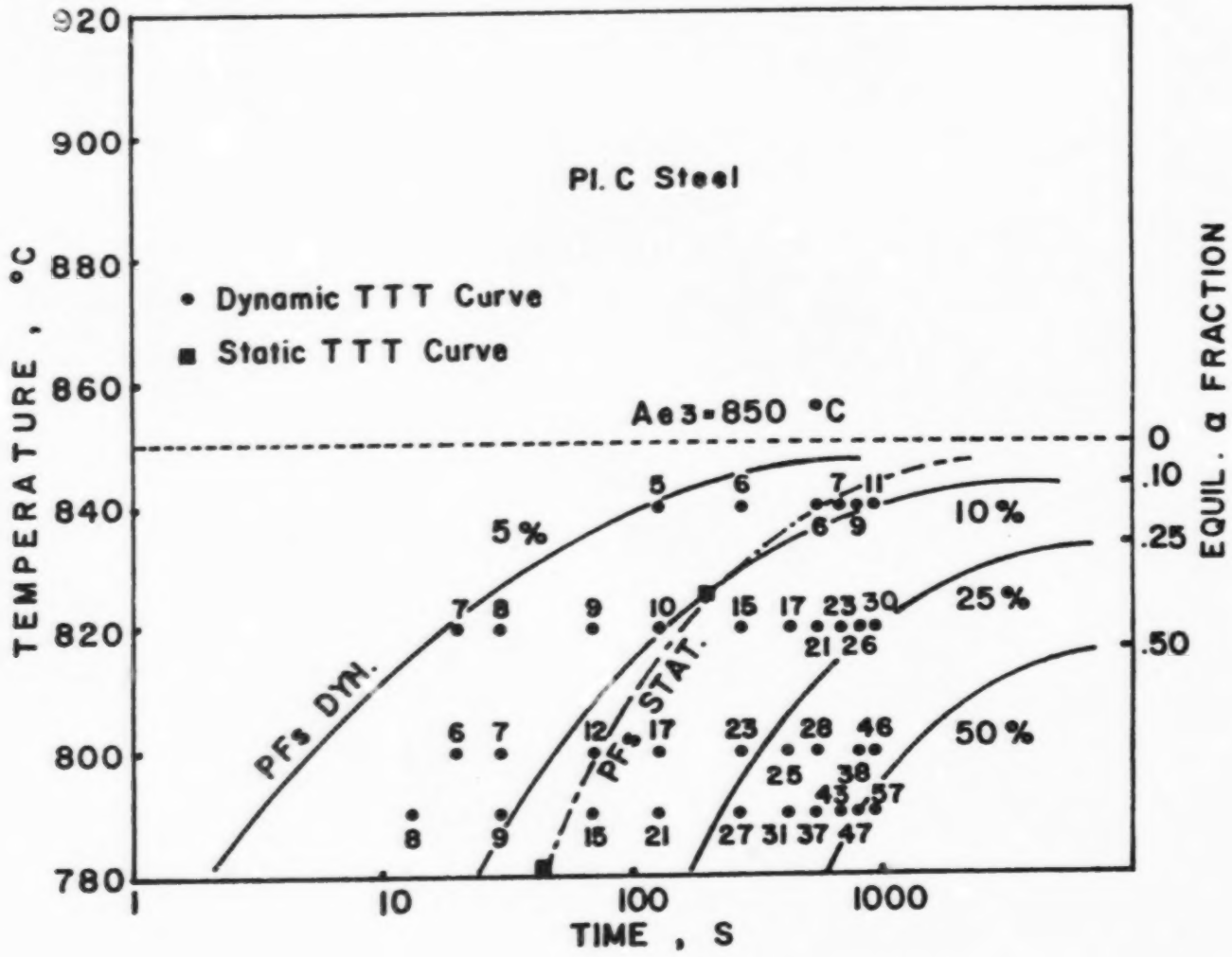

Figure 6 TTT characteristics of the plain C steel.

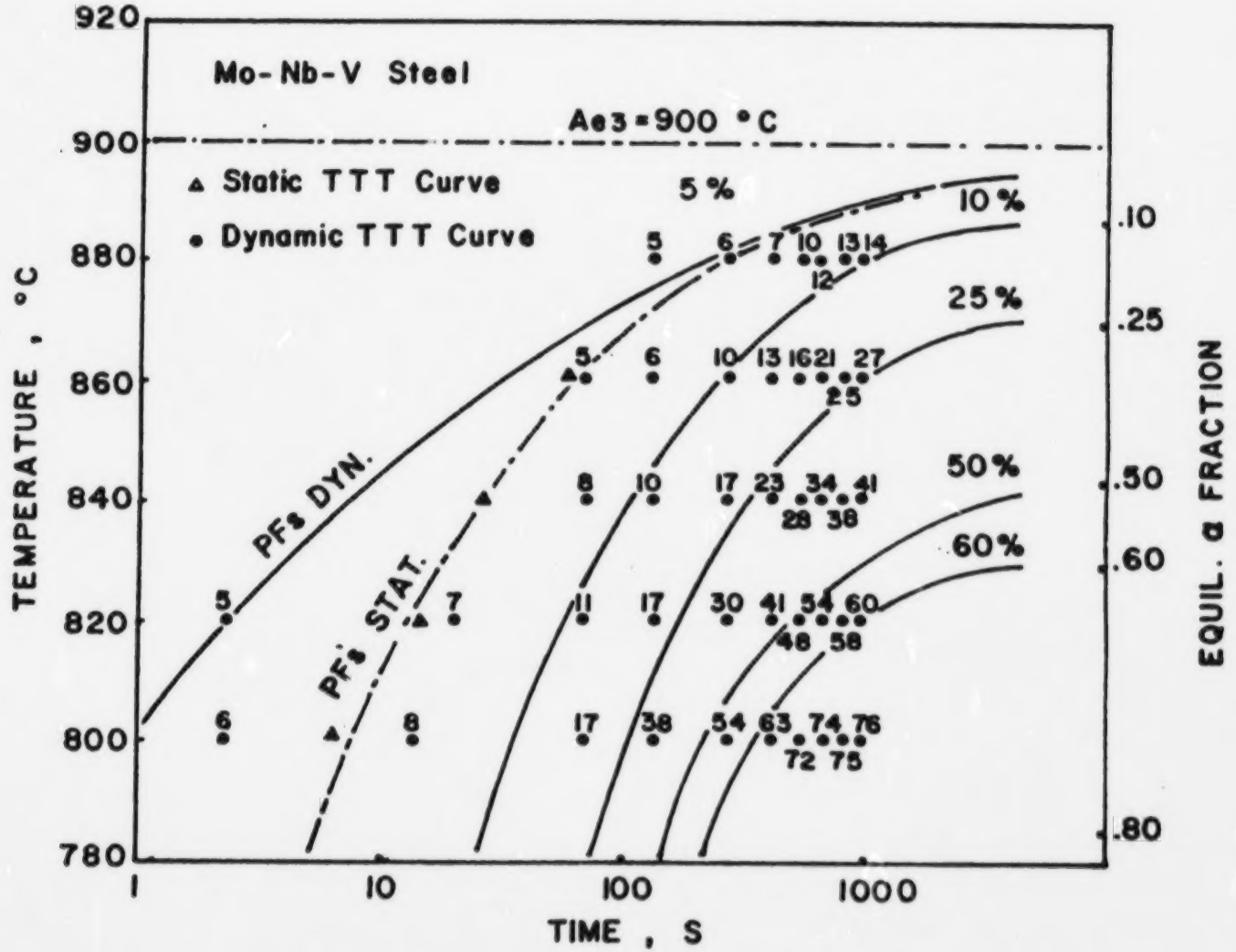

Figure 8 TTT characteristics of the Mo-Nb-V steel.

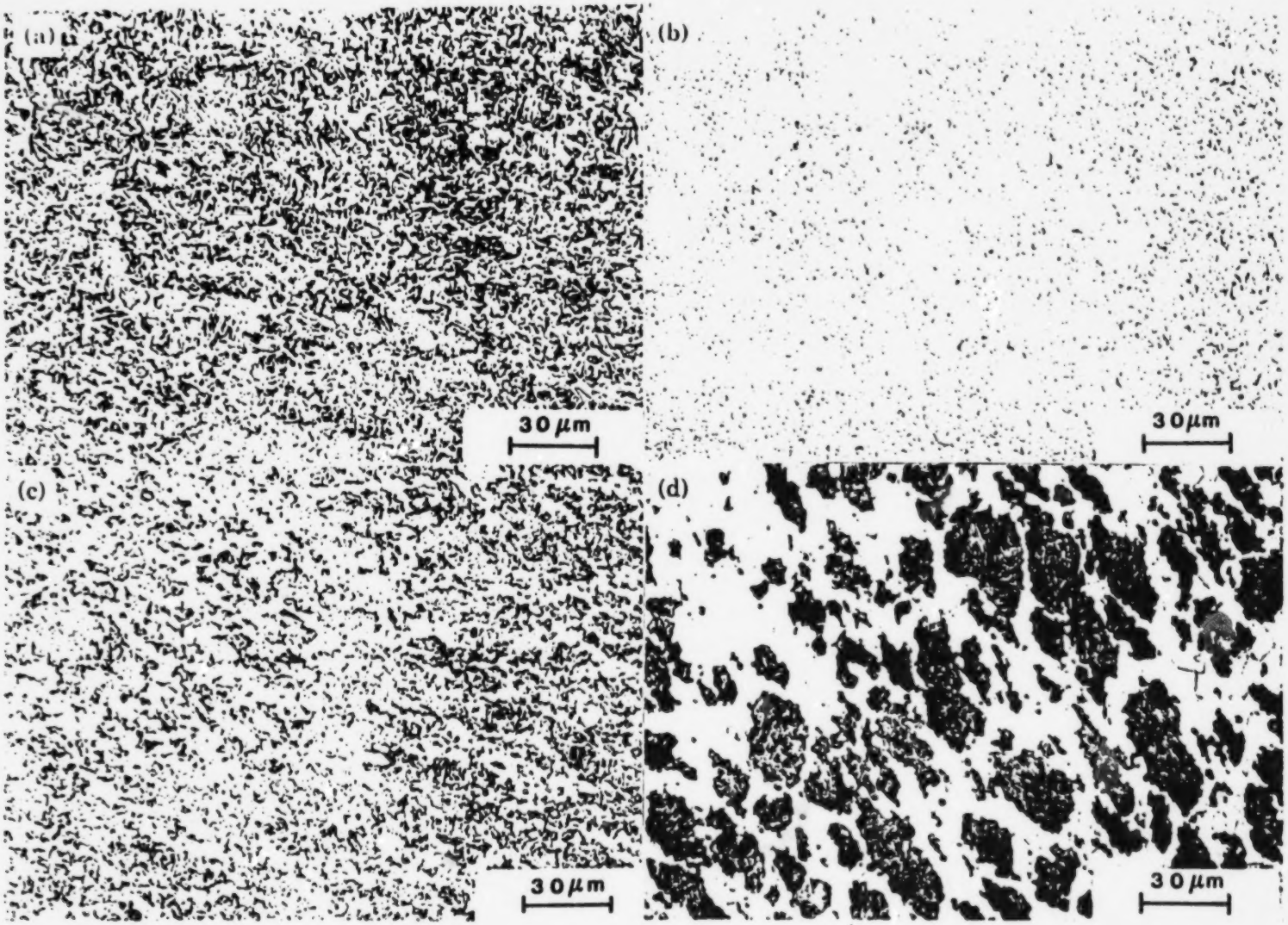

Figure 9 Microstructure of Mo steel samples deformed at 800°C and water quenched.
(a) deformed for 1 s to $\varepsilon = 0.8$ at a constant strain rate of 7.4×10^{-1} s^{-1}; 27% PF;
(b) deformed for 11 s to $\varepsilon = 0.8$ at a constant strain rate of 7.4×10^{-2} s^{-1}; 34% PF;
(c) deformed for 116 s to $\varepsilon = 0.8$ at a constant strain rate of 7.4×10^{-3} s^{-1}; 46.5% PF;
(d) deformed for 1167 s to $\varepsilon = 0.8$ at a constant strain rate of 7.4×10^{-4} s^{-1}; 52% PF.

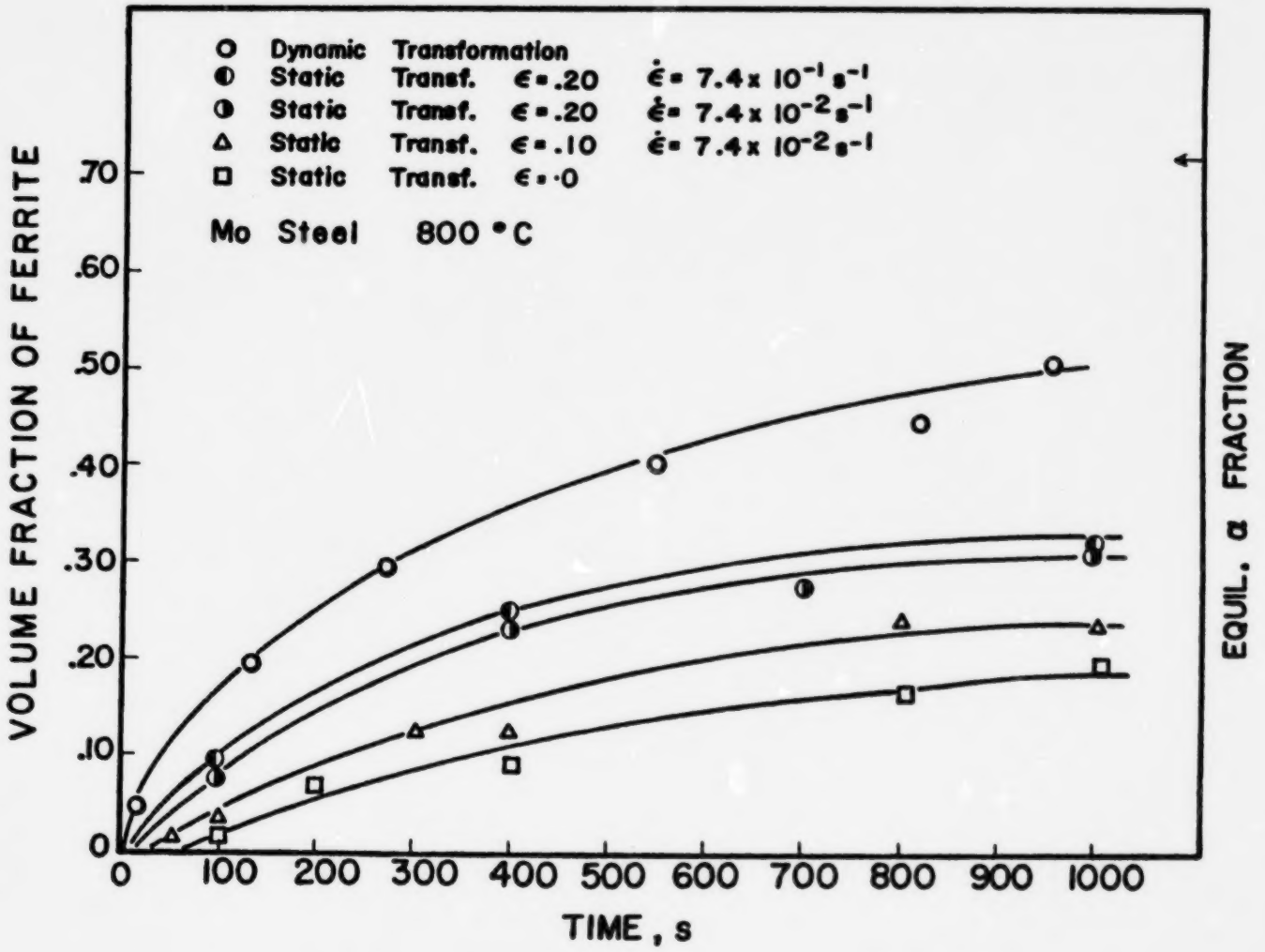

Figure 10 Effect of prestrain and strain rate on the austenite to ferrite transformation at 800°C in the Mo steel.

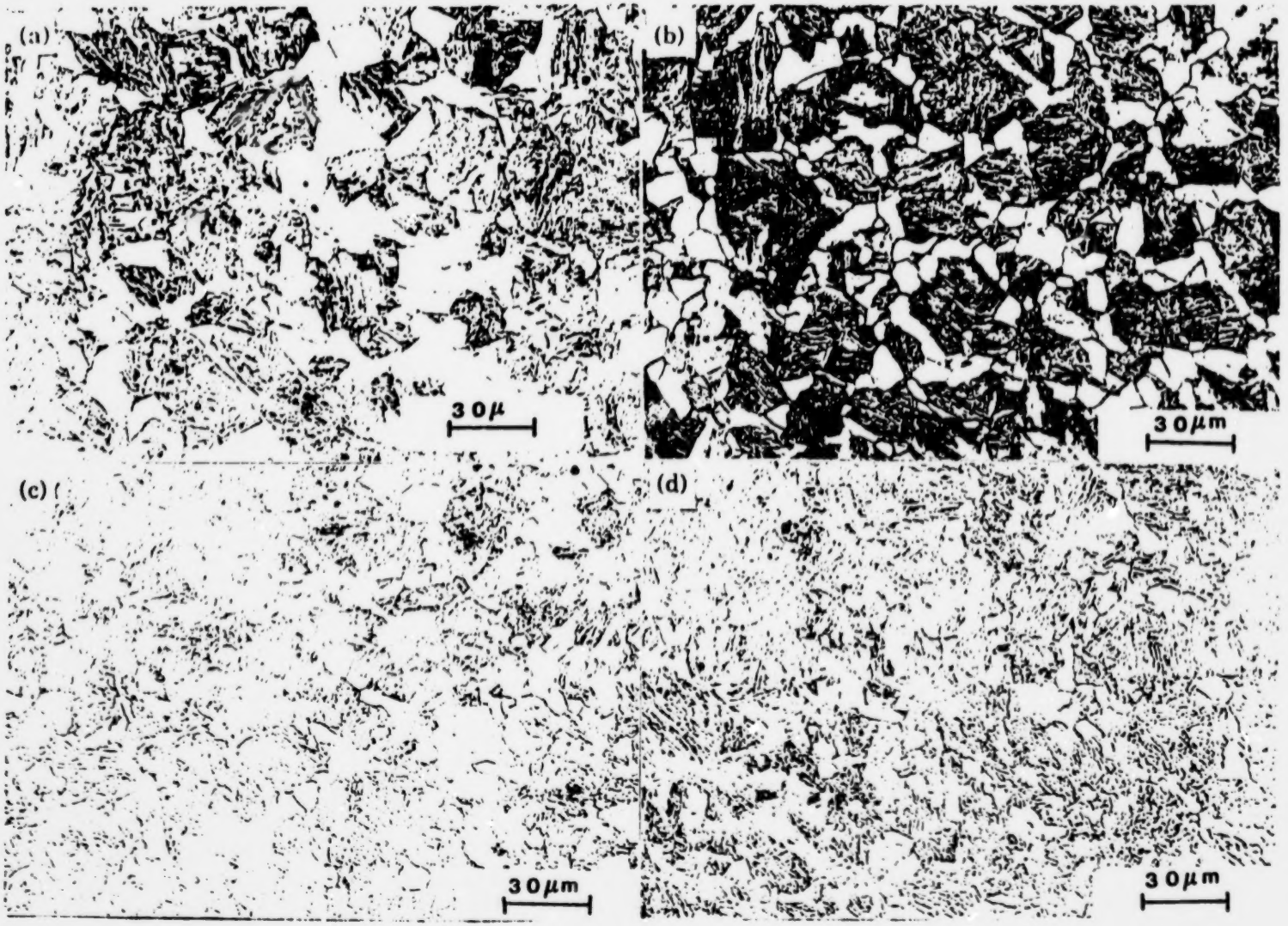

Figure 11 Microstructure of Mo steel samples held for 1000 s at 800°C and water quenched. (a) No deformation; 18%PF; (b) Prestrained to $\varepsilon = 0.10$ at $\dot{\varepsilon} = 7.4 \times 10^{-2}\ s^{-1}$; 22% PF; (c) Prestrained to $\varepsilon = 0.20$ at $\dot{\varepsilon} = 7.4 \times 10^{-2}\ s^{-1}$; 30% PF; (d) Prestrained to $\varepsilon = 0.20$ at $\dot{\varepsilon} = 7.4 \times 10^{-1}\ s^{-1}$; 31% PF.

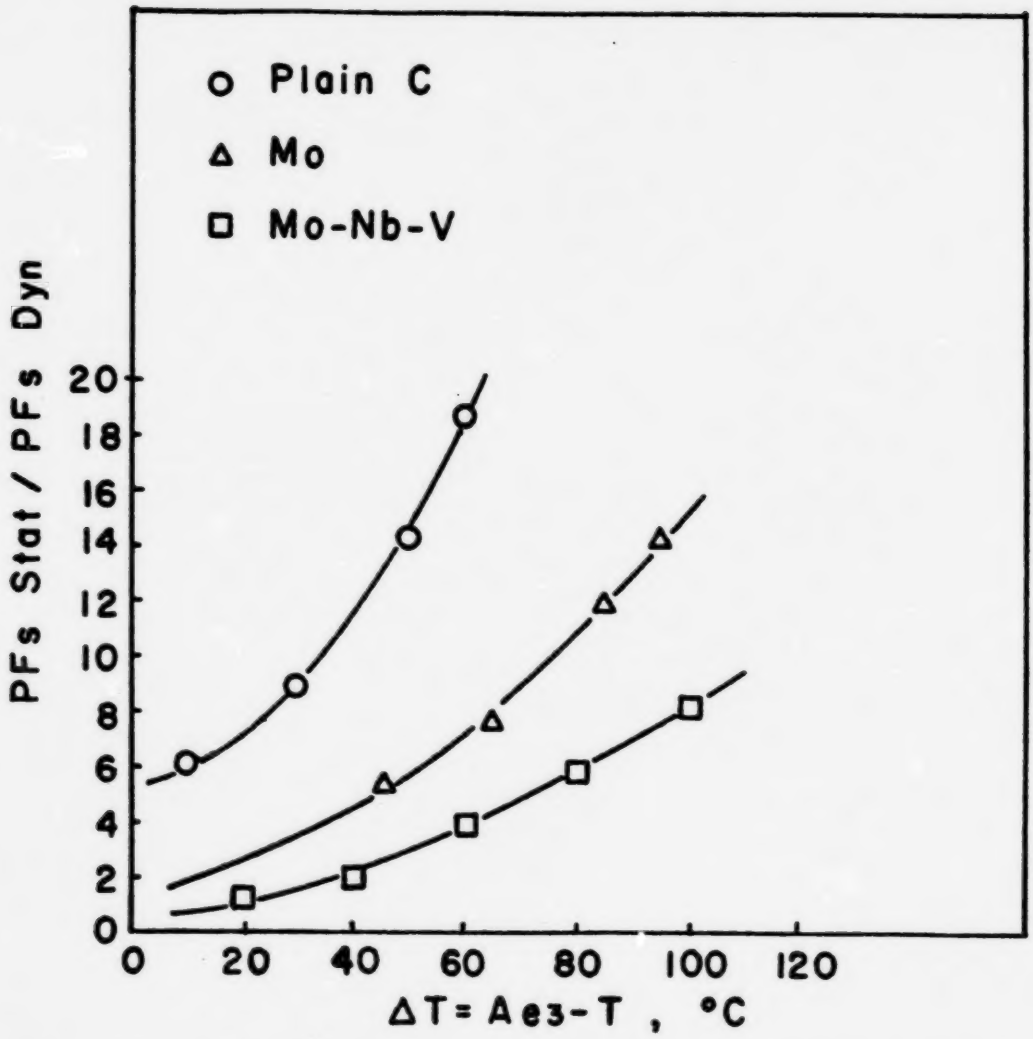

Figure 13 Effect of degree of undercooling on the polygonal ferrite start time in the three steels.

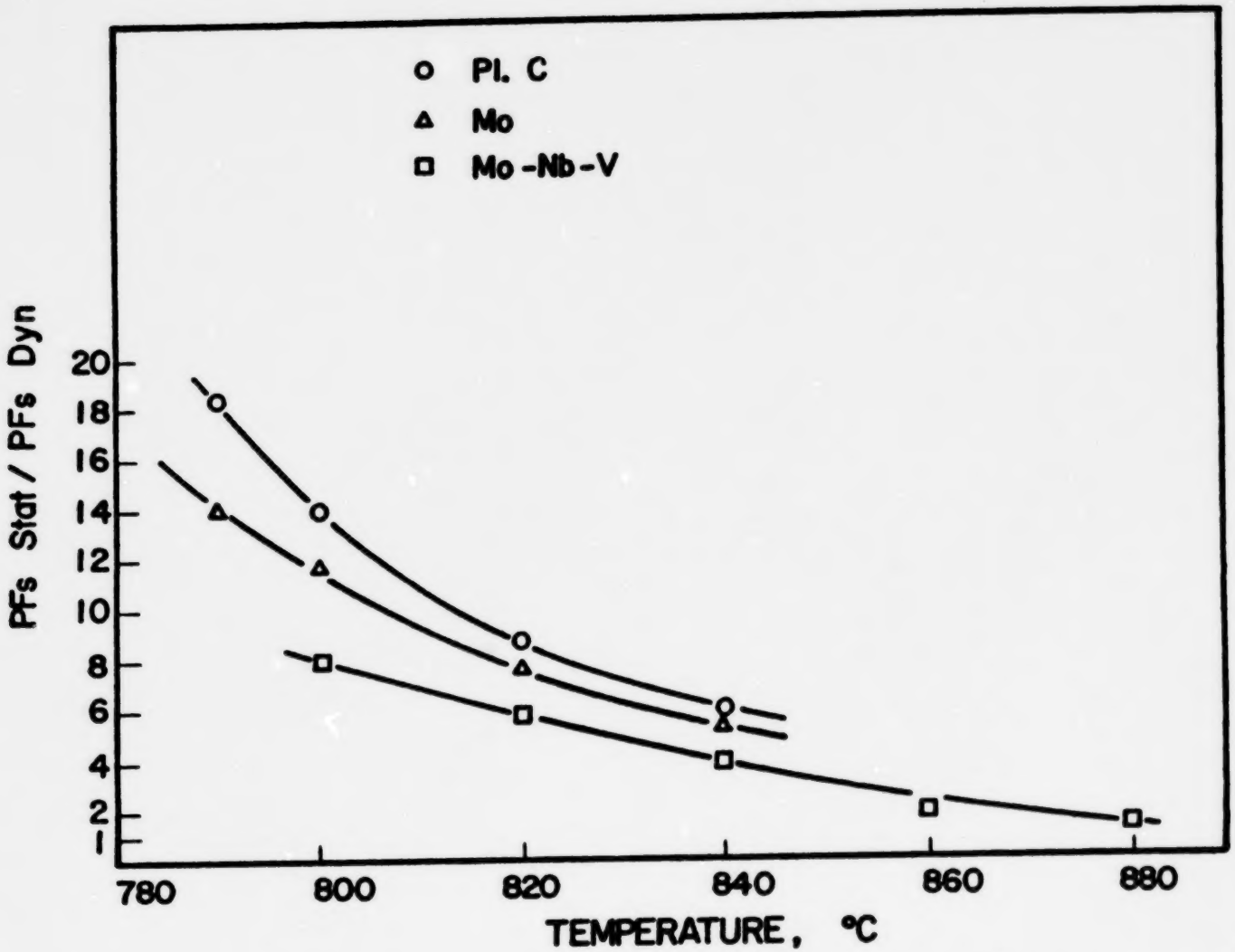

Figure 12 Effect of deformation on the polygonal ferrite start time for the plain C, Mo and Mo-Nb-V steels.